Vision Research 50 (2010) 2176–2187

Contents lists available at ScienceDirect

Vision Research

journal homepage: www.elsevier.com/locate/visres

ERG changes in albino and pigmented mice after optic nerve transection

Luis Alarcón-Martínez [a,1], Marcelino Avilés-Trigueros [a,1], Caridad Galindo-Romero [a], Javier Valiente-Soriano [a], Marta Agudo-Barriuso [c], Pedro de la Villa [b], Maria P. Villegas-Pérez [a], Manuel Vidal-Sanz [a,*]

[a] Departamento de Oftalmología, Facultad de Medicina, Universidad de Murcia, 30100 Murcia, Spain
[b] Departamento de Fisiologia, Facultad de Medicina, Universidad de Alcalá, 28871 Alcalá de Henares, Spain
[c] Unidad de Investigación, Hospital Universitario Virgen de la Arrixaca, Servicio Murciano de Salud, Fundación para la Formación e Investigación Sanitarias de la Región de Murcia, 30120 Murcia, Spain

ARTICLE INFO

Article history:
Received 2 June 2010
Received in revised form 12 August 2010

Keywords:
Electroretinogram (ERG)
Scotopic threshold response (STR)
Optic nerve transection (ONT)
Axotomy
Retinal ganglion cells (RGCs)
Adult albino and pigmented mice
Neuronal degeneration
Retina

ABSTRACT

Optic nerve transection (ONT) triggers retinal ganglion cell (RGC) death. By using this paradigm, we have analyzed for the first time in adult albino and pigmented mice, the effects of ONT in the scotopic threshold response (STR) components (negative and positive) of the full-field electroretinogram. Two weeks after ONT, when in pigmented mice approximately 18% of the RGC population survive, the STR-implicit time decreased and the p and nSTR waves diminished approximately to 40% or 55%, in albino or pigmented, respectively, with respect to the values recorded from the non-operated contralateral eyes. These changes were maintained up to 12 weeks post-ONT, demonstrating that the ERG–STR is a useful parameter to monitor RGC functionality in adult mice.

1. Introduction

In response to a flash of light the electrical response than can be recorded at the cornea is known as the electroretinogram (ERG) (Dowling, 1987; Frishman, 2006). The ERG is formed by different individual components that can be associated to their cells of origin. The initial negative wave recorded after a bright full-field stimulus (the so named *a*-wave) is accepted to be generated by photoreceptor phototransduction, while the prominent positive wave that follows the *a*-wave (so named *b*-wave) is mainly generated by depolarization of ON-bipolar cells and Müller cells (Dowling, 1987; Frishman, 2006). In addition to the *a*- and *b*-waves, other main components of the ERG that appear superimposed on the *b*-wave are the oscillatory potentials which are thought to arise from feedback circuitries as well as from amacrine cells (Wachtmeister, 1998).

When very dim light stimuli are presented in scotopic conditions a small cornea-negative potential, called negative scotopic threshold response (nSTR) (Sieving, Frishman, & Steinberg, 1986), dominates the ERG. The nSTR has been recorded in humans (Frishman, Reddy, & Robson, 1996; Korth, Nguyen, Horn, & Martus, 1994; Sieving & Nino, 1988), cats (Sieving et al., 1986), monkeys (Frishman, Shen, et al., 1996), rats (Alarcón-Martínez et al., 2009; Bui & Fortune, 2004) and mice (Saszik, Frishman, & Robson, 2002). Intraretinal recordings (Frishman & Steinberg, 1989a, 1989b; Sieving et al., 1986) and studies with pharmacological substances (Naarendorp & Sieving, 1991; Robson & Frishman, 1995; Saszik et al., 2002) have indicated that this potential corresponds to inner retina neurons; amacrine and/or ganglion cells. Moreover, there is a cornea-positive component forming the STR (pSTR), and this is abolished with pharmacological agents inhibiting the response of the inner retina (Naarendorp & Sieving, 1991; Saszik et al., 2002).

Intraorbital optic nerve transection (ONT) is a classic model to study injury-induced RGC regenerative and degenerative responses (Aguayo, Vidal-Sanz, Villegas-Pérez, & Bray, 1987; Avilés-Trigueros, Sauvé, Lund, & Vidal-Sanz, 2000; Vidal-Sanz, Bray, & Aguayo, 1991; Vidal-Sanz, Bray, Villegas-Perez, Thanos, & Aguayo, 1987; Vidal-Sanz, Villegas-Perez, Bray, & Aguayo, 1993; Vidal-Sanz et al., 2000; Whiteley, Sauvé, Avilés-Trigueros, Vidal-Sanz, & Lund, 1998), including cell loss (Nadal-Nicolás et al., 2009; Parrilla-Reverter, Agudo, Sobrado-Calvo, et al., 2009; Peinado-Ramón, Salvador, Villegas-Pérez, & Vidal-Sanz, 1996; Villegas-Pérez, Vidal-Sanz, Bray, & Aguayo, 1988; Villegas-Pérez, Vidal-Sanz, Rasminsky, Bray, &

* Corresponding author. Address: Departamento de Oftalmología, Facultad de Medicina, Universidad de Murcia, Campus de Espinardo, E-30100 Espinardo, Murcia, Spain. Fax: +34 968 363962.
E-mail address: ofmmv01@um.es (M. Vidal-Sanz).
[1] These authors contributed equally to this work.

0042-6989/$ - see front matter © 2010 Elsevier Ltd. All rights reserved.
doi:10.1016/j.visres.2010.08.014

Aguayo, 1993). In adult rats, ONT induces within 2 weeks the loss of approximately 80% of the RGC population, while the remaining RGCs undergo a slower degeneration rate (Villegas-Pérez et al., 1993). ONT also results in a number of alterations in their functional (Casson, Chidlow, Wood, Vidal-Sanz, & Osborne, 2004; McKerracher, Vidal-Sanz, & Aguayo, 1990; McKerracher, Vidal-Sanz, Essagian, & Aguayo, 1990; Parrilla-Reverter, Agudo, Nadal-Nicolás, et al., 2009; Schlamp, Johnson, Li, Morrison, & Nickells, 2001) and metabolic (Chidlow, Casson, Sobrado-Calvo, Vidal-Sanz, & Osborne, 2005; Lindqvist, Peinado-Ramónn, Vidal-Sanz, & Hallböök, 2004; Lindqvist, Vidal-Sanz, & Hallböök, 2002; Lindqvist et al., 2010) properties, as well as in the regulation of a substantial number of genes (Agudo et al., 2008, 2009). This experimental model appears suitable to study the ERG components generated by the RGC population in adult mammals because, it is widely accepted that ONT results in selective loss of RGCs but not of other non-RGC retinal neurons (Carter, Vidal-Sanz, & Aguayo, 1987; Villegas-Pérez et al., 1993) or in the impairment of the outer retinal neurons functionality (Alarcón-Martínez et al., 2009; Bui & Fortune, 2004).

There is a number of studies in rats analyzing the electroretinographic responses after ONT (Alarcón-Martínez et al., 2009; Bui & Fortune, 2004; Mojumder, Sherry, & Frishman, 2008), however such information is lacking for mice. Transgenic and knock-out mice have become an important tool to study a number of relevant questions in the adult mammalian visual system. Moreover, albino or pigmented mice are usually the animal of choice for many experimental models involving RGC injury, including ocular hypertension induced by laser photocoagulation of the limbar tissues (Cuenca et al., 2010; Fu & Sretavan, 2010; Grozdanic et al., 2003; Holcombe, Lengefeld, Gole, & Barnett, 2008; Morrison, Johnson, & Cepurna, 2008; Salinas-Navarrov, Alarcón-Martínez, et al., 2009; Salinas-Navarro et al., 2010), thus it is important to ascertain the origin of the STR waves in this species. In the present work we have studied the ERG response after ONT at different time intervals for albino and pigmented mice to provide further evidence for the relationship between the generation of the STR components of the full-field electroretinogram and the anatomical integrity of the RGC population. Using a classic model of axotomy-induced RGC injury, we have investigated in adult albino and pigmented mice the different components of the full-field flash ERG at various time intervals after ONT as well as RGC survival. Retrogradely transported neuronal tracers were applied to both superior colliculi (SCi) to identify RGCs, and we report that optic nerve (ON) injury results by 2 weeks in the loss of approximately 80% of the RGC population. Moreover, ONT resulted in major permanent reductions of the early components of the ERG, mainly the positive scotopic threshold response, and alterations of the STR-implicit time. Overall, our data provide new and original information for the electrophysiology of the adult albino and pigmented mice after ONT and document that ERG STR could be a useful parameter to monitor RGC functionality in adult mice (short accounts of this work have been published in abstract format; Alarcón-Martínez et al., 2010; Galindo-Romero et al., 2010).

2. Materials and methods

2.1. Animals

Female adult albino (BALB/c; 30–35 g) and pigmented (C57BL/6; 30–35 g) mice of the same age were treated according to institutional guidelines, European Union regulations for the use of animals in research, the ARVO statement for the use of animals in ophthalmic and vision research, and were comparable to those published by the Institute for Laboratory Animal Research (Guide for the Care and Use of Laboratory Animals). Mice were anaesthetized with an intraperitoneal (i.p.) injection of a mixture of ketamine (70 mg/kg Ketolar®, Pfizer, Alcobendas, Madrid, Spain) and xylazine (10 mg/kg Rompur®, Bayer, Kiel, Germany) in 0.1 ml saline. Mice were kept in a 12-h light/dark cycle. For electrophysiological studies, three groups of albino mice; group I ($n = 9$), II ($n = 6$) or III ($n = 5$), were processed at 2, 4 or 12 weeks after ONT, respectively, and three groups of pigmented mice; group IV ($n = 7$), V ($n = 6$) or VI ($n = 9$) were processed at 2, 4 or 12 weeks

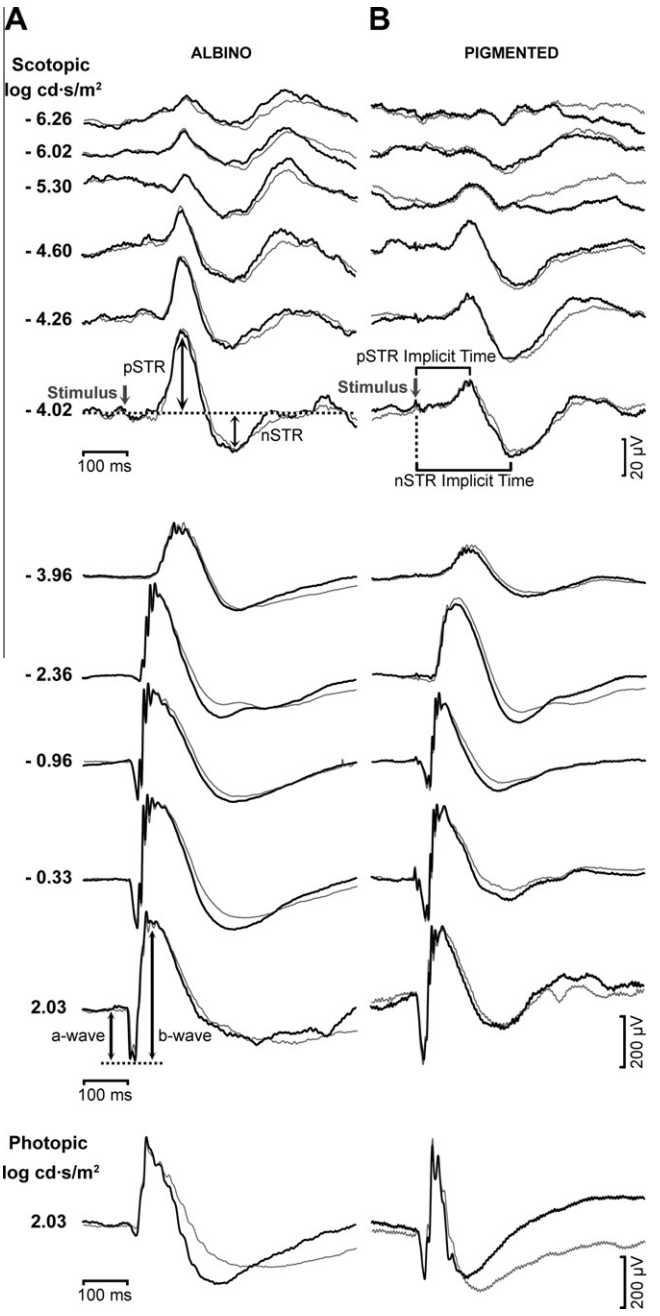

Fig. 1. Scotopic and photopic electroretinographic recordings in albino and pigmented mice. Examples of the ERG traces recorded in an albino (A) or pigmented (B) control mouse in response to flash stimuli of increasing intensity (indicated in log cd s/m^2 units at the left of the recording traces) for the right eye (thin trace) and for the left eye (bold trace). The scotopic threshold responses (STR) were elicited by weak light stimuli (−6.26 to −4.02 log cd s/m^2). Responses mediated by rods and by rods and cones (mixed response) were elicited by light intensities from −3.96 to 2.03 log cd s/m^2. Photopic response was recorded after a light adaptation of 5 min and it was elicited by the highest light stimulus (2.03 log cd s/m^2). No significant differences in the ERG amplitudes between left and right eyes were observed. Examples for the measurement of wave amplitudes and implicit times are shown.

after ONT, respectively. For anatomical studies a group of pigmented mice; group VII ($n = 8$) processed at 2 weeks after ONT and an additional control group VIII ($n = 8$) was used.

2.2. Intraorbital optic nerve transection (ONT)

The left ON was sectioned close to its origin in the optic disk following previously described protocols that are standard in our Laboratory (Salinas-Navarro et al., 2010; Vidal-Sanz et al., 1987). In brief, to access the ON at the back of the eye, an incision was made in the skin overlying the superior orbital rim, the supero-external orbital contents were dissected, and the superior and external rectus muscles were sectioned. The duramater of the ON was opened longitudinally, and the ON was transected completely as close as possible to the eye. Care was taken not to damage the retinal blood supply, which enters the eye separately in the inferonasal aspect of the ON sheath.

2.3. Electroretinography

Animals were dark adapted overnight prior to ERG recordings and their manipulation was done under dim red light ($\lambda > 600$ nm). Mice were anaesthetized and bilateral pupil midriasis was induced by applying in both eyes a topical drop of 1% tropicamide (colircusi tropicamida 1%®; Alcon-Cusí, S.A., El Masnou, Barcelona, Spain). The light stimulation device consisted in Ganzfeld dome, which ensures a homogeneous illumination anywhere in the retina, with multiple reflections of the light generated by light emitting diodes (LED), which provided a wide range of light intensities. For high intensity illuminations, a single LED placed close (1 mm) to the eye was used. Light intensity was calibrated by a dual-biosignal generator device specifically adapted for ERG responses. The recording system was composed by mouse Burian–Allen bipolar electrodes (active and reference electrode placed in the eye and mouth respectively) (Hansen Labs, Coralville, IA, USA) with a corneal contact shape; a drop of methylcellulose, 2% (methocel 2%®; Novartis Laboratories CIBA Vision, Annonay, France) was placed between the eye and the electrode to maximize conductivity of the generated response. The ground electrode was placed in the tail. Electrical signals generated in the retina were amplified (1000×) and filtered (band pass from 1 Hz to 1000 Hz) by the use of commercial amplifier (Digitimer Ltd., Letchworth Garden City, UK). The recorded signals were digitized (Power Lab; ADInstruments Pty. Ltd., Chalgrove, UK) and displayed on a PC computer. Bilateral ERG recording were performed simultaneously from both eyes. Light stimuli were calibrated before each experiment and the calibration protocol assured the same recordings parameters for both eyes. The ERG responses were recorded by stimulating the retina with light intensities ranged between 10^{-6} and 10^{-4} cd s m^{-2} for the scotopic threshold response (STR), 10^{-4} and 10^{-2} cd s m^{-2} for the response mediated by rods and between 10^{-2} and 10^{2} cd s m^{-2} for the mixed (mediated by rods and cones) response. After 5 min of a light adaptations the photopic responses were recorded by the highest stimulus (10^{2} cd s m^{-2}). For each light intensities, a series of ERG responses were averaged (from a number of 40 ERG responses for the dimmest stimulus intensity to a number of 5 for the brightest stimulus) and the interval between light flashes was adjusted to appropriate times that allowed response recovering (from 5 s for the dimmest stimulus intensities to 60 s for the brightest stimulus). At the end of each session the animals were treated with topical tobramicine (Tobrex®; Alcon-Cusí, S.A., El Masnou, Barcelona, Spain) in both eyes. The analysis of the different recordings was performed with the normalization criteria established for the ISCEV for the measures of the amplitude and implicit time of the different waves which were studied (Fig. 1).

2.4. Functional analysis

The STR was analyzed for each stimulus; pSTR was measured from baseline to the "hill" of the positive deflection, approximately 110 ms from the flash onset, and nSTR was measured from baseline

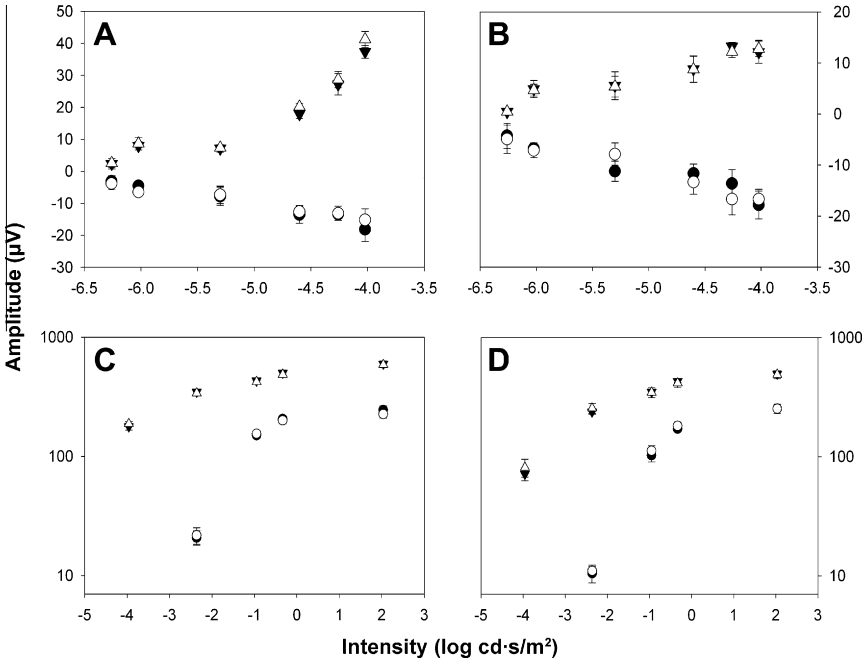

Fig. 2. Electroretinographic amplitude measurements in albino and pigmented mice. Averaged data (mean ± SEM) of ERG amplitudes versus stimulus intensities both from control albino (A and C; $n = 6$) and pigmented mice (B and D; $n = 6$) is shown for the right eye (open symbols) and left eye (filled symbols). (A and B) negative scotopic threshold response (circles) and positive scotopic threshold responses (triangles). (C and D) *a*-wave (circles) and *b*-wave (triangles). No significant differences were observed between mice strains except for the pSTR amplitude which was higher for albino mice (*t*-test; $P < 0.05$).

to first "valley" after pSTR, approximately 220 ms from the flash onset. The *a*-wave was measured from the baseline to the first valley, approximately 10 ms, from the flash onset and the *b*-wave amplitude was measured from the bottom of the *a*-wave valley to the top of the hill of the positive deflection; the time point of the *b*-wave measurement, varied depending of the intensity used. The implicit time was measured for each wave, from the presentation of the stimulus to the maximum of the waves. Data from operated and non-operated eyes were compared; ERG wave amplitudes and implicit times were calculated for each animal group and the percentage of difference between the operated and the non-operated eyes were obtained for each stimulus and further averaged (mean ± SEM). The results were analyzed with SigmaStat® 3.1 for Windows® (Systat Software, Inc., Richmond, CA, USA). Descriptive statistics were calculated, the normality of the distribution of the data was examined with a normality test and parametric or non-parametric test were used accordingly; *t*-test was used for the comparison between the absolute response of both eyes prior and post-ONT and for the comparison of the per cent response of the operated eye respect the control eye, prior and post-ONT. ANOVA on ranks test were used to compare the per cent response between different animal groups and the difference of the implicit time between experimental and control eyes along the different groups too, as an attempt to estimate a possible interrelation between the progressions of response along studied times. The statistic significance was placed in a $P < 0.05$ for all tests and the statistic was always of two tails.

2.5. Retrograde tracing

To identify the population of RGCs, hydroxystilbamidine methanesulfonate (OHSt) was applied, 1 week before surgery (experimental retinas) or processing (control group), to both superior colliculi (SCi) in C57 adult mice where 96.6% of the RGC axons project (see Tables 3 and 4 in Salinas-Navarro, Jiménez-López, et al., 2009). In brief, after exposing the midbrain, a small pledget of gelatin sponge (Espongostan® Film, Ferrosan A/S, Denmark) soaked in saline containing 10% DMSO and 10% OHSt, a small (472,53 kDa Mw) molecule (Molecular Probes, Leiden, The Netherlands) with similar fluorescent and tracer properties to fluorogold (Cheunsuang & Morris, 2005), was applied over the entire surface of both SCi, following previously described methods that are standard in our laboratory (Salinas-Navarro, Jiménez-López, et al., 2009; Salinas-Navarro, Mayor-Torroglosa, et al., 2009; Salinas-Navarro, Alarcón-Martínez, et al., 2009; Salinas-Navarro et al., 2010; Vidal-Sanz, Villegas-Perez, Bray, & Aguayo, 1988; Wang, Villegas-Pérez, Vidal-Sanz, & Lund, 2000; Wang et al., 2003).

2.6. Histology and retinal analysis

Mice were deeply anesthetized, perfused transcardially through the ascending aorta with saline and then with 4% paraformaldehyde in 0.1 M phosphate buffer (PB) (pH 7.4). Special care was taken to maintain the orientation of each eye, and right after deep anesthesia and before perfusion fixation a suture was placed on the superior pole of each eye. Upon dissection of the eyeball, the rectus muscle insertion into the superior part of the eye and the nasal caruncle were used as additional landmarks. Both retinas were dissected and prepared as flattened whole-mounts by making four radial cuts (the deepest one in the superior pole), post-fixed for an additional hour, rinsed in 0.1 M PB, mounted vitreal side up on subbed slides and covered with anti-fading mounting media containing 50% glycerol and 0.04% p-phenylenediamine in 0.1 M sodium carbonate buffer (pH 9).

All whole mounted retinas (left and right eyes) were analyzed to identify OHSt–labeled RGCs. To make reconstructions of retinal whole-mounts, the retinas were photographed under an epifluorescence microscope (Axioscop 2 Plus; Zeiss Mikroskopie, Jena, Germany) equipped with a computer-driven motorized stage (ProScan™ H128 Series, Prior Scientific Instruments, Cambridge, UK), controlled by IPP (IPP 5.1 for Windows®; Media Cybernetics, Silver Spring, MD, USA) as previously described (Salinas-Navarro, Jiménez-López, et al., 2009; Salinas-Navarro, Mayor-Torroglosa,

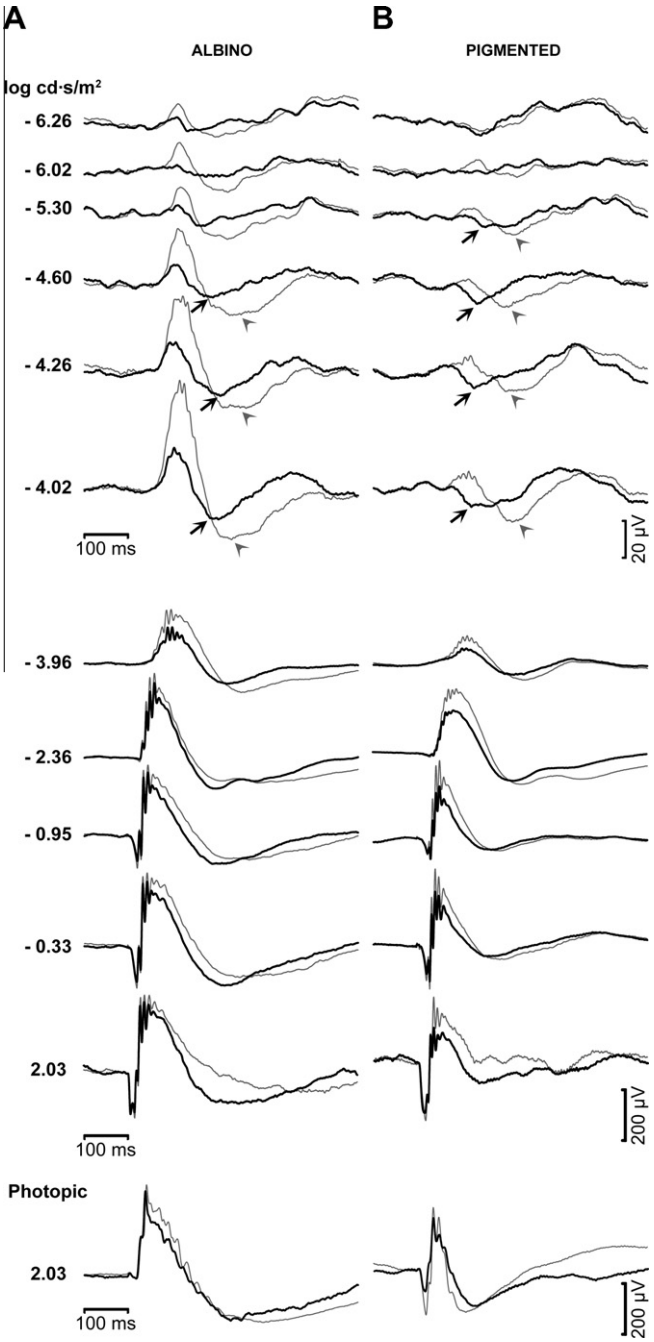

Fig. 3. Scotopic and photopic electroretinographic recordings 2 weeks after optic nerve transection. Examples of the ERG traces recorded in an albino (A) and pigmented (B) mouse in response to flash stimuli of increasing intensity for the non-operated right eye (thin traces) and the operated left eye (bold traces) 2 weeks after ONT. The intensity of the flash stimuli is indicated to the left of the recording traces. Reduction in the nSTR and pSTR responses from operated eyes versus control eyes is clearly observed both in albino and pigmented mice. The STR-implicit time of the operated eye (arrows) is also altered respect to the non-operated eye (arrow heads). The *a*- and *b*-wave of the operated eye are slightly decreased respect to the non-operated eye.

et al., 2009; Salinas-Navarro, Alarcón-Martínez, et al., 2009; Salinas-Navarro et al., 2010). Reconstructed whole-mounts, made up from 140 individual frames, were further processed when required using Adobe Photoshop® CS 8.0.1 (Adobe Systems, Inc., San Jose, CA, USA).

The individual OHSt-fluorescent images taken for each retinal whole-mount were processed with a specific cell-counting subroutine developed by our group (Salinas-Navarro, Jiménez-López, et al., 2009; Salinas-Navarro, Mayor-Torroglosa, et al., 2009) and this method was used to automatically quantify OHSt$^+$–RGCs in naïve or control uninjured right retinas. To determine the number of OHSt$^+$–RGCs in injured retinas at 2 weeks, these were manually counted following previously described methods (Gómez-Ramírez,

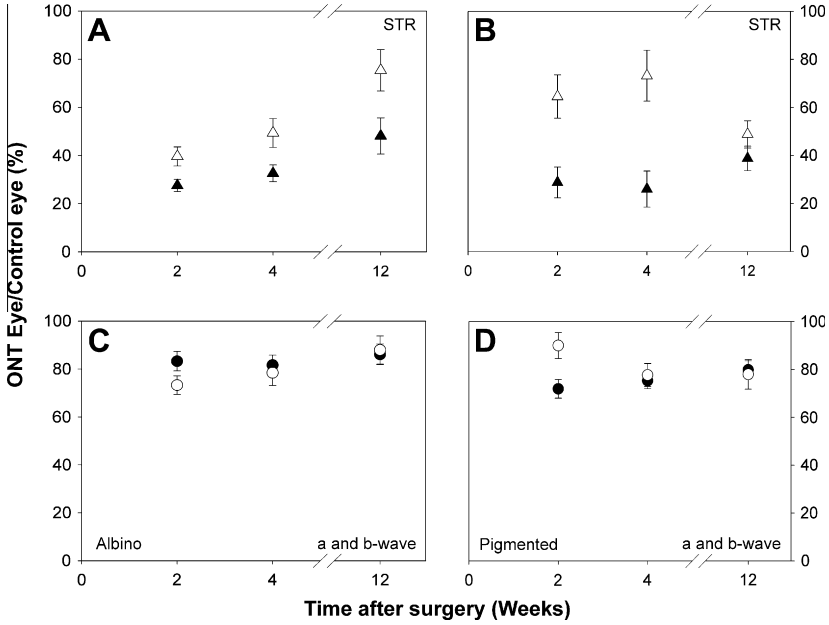

Fig. 4. Evolution of electroretinographic wave amplitudes along 12 weeks time period. Average data (mean ± SEM) of the reduction in the ERG wave amplitudes is represented as the percentage between operated and non-operated eyes for 2, 4 and 12 weeks after ONT, both from albino (A and C) and pigmented mice (B and D). (A and B) negative scotopic threshold amplitude (open triangles) and positive scotopic threshold amplitude (closed triangles). (C and D) *a*-wave (open circles) and *b*-wave (closed circles). A permanent high reduction in the pSTR and nSTR is observed for the 12 weeks time period in both mice strains. On the other hand, *a*-wave and *b*-wave amplitudes are close to the normal values for all experiment.

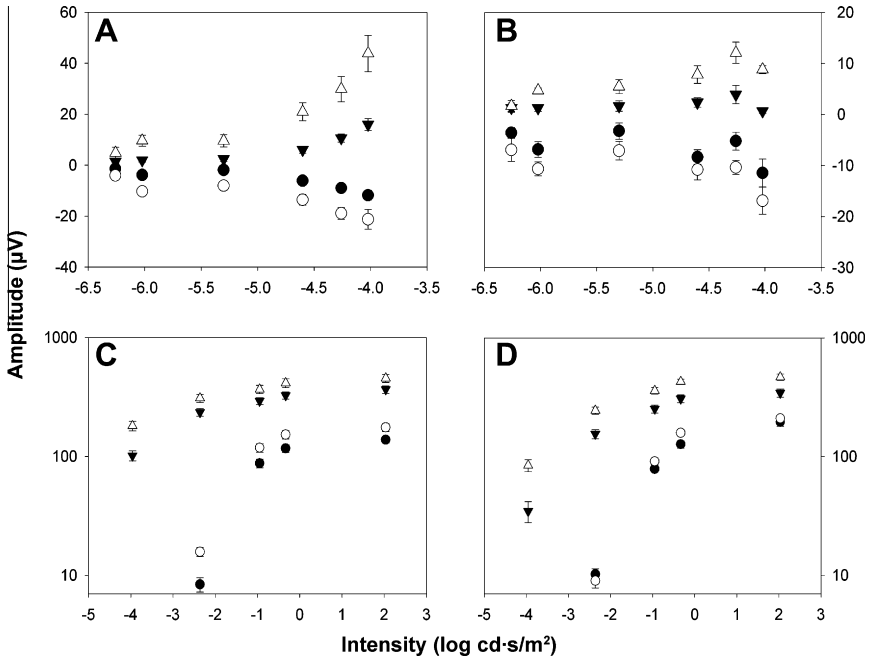

Fig. 5. Electroretinographic amplitude measurements 2 weeks after optic nerve transection. Averaged data (mean ± SEM) of ERG amplitudes versus stimulus intensity both from albino (A and C; $n = 9$) and pigmented mice (B and D; $n = 7$) from recordings obtained 2 weeks after ONT from non-operated right eye (open symbols) and operated left eye (filled symbols). (A and B) negative scotopic threshold responses (circles) and positive scotopic threshold responses (triangles). (C and D) *a*-wave (circles) and *b*-wave (triangles). A significant reduction of the wave amplitudes of the nSTR and pSTR is observed in the operated eyes (*t*-test; $P < 0.05$). Moreover, a mild decrease in the *b*-wave scotopic response and *a*- and *b*-wave is also observed in the operated eyes (*t*-test; $P < 0.05$) versus control eyes.

Villegas-Pérez, Miralles de Imperial, Salvador-Silva, & Vidal-Sanz, 1999; Nadal-Nicolás et al., 2009; Parrilla-Reverter, Agudo, Sobrado-Calvo, et al., 2009; Salvador-Silva, Vidal-Sanz, & Villegas-Pérez, 2000; Vidal-Sanz, Lafuente, Mayor, de Imperial, & Villegas-Pérez, 2001) because the presence of microglial cells transcellularly labeled with OHSt interfered with the automatic counting (Nadal-Nicolás et al., 2009). The fusiform body and the dot-like OHSt accumulations in microglial cells made it possible to distinguish them from the typical appearance of OHSt$^+$–RGCs (Vidal-Sanz et al., 2001). In brief: OHSt$^+$–RGCs were counted by two investigators blinded to the procedure, from photographs of 12 rectangular areas (each of 0.1515 mm^2) of each retina, three in each quadrant. The first image was taken at 0.875 mm from the optic disk and the remaining two 1 mm apart from each other. The number of labeled cells in the 12 photographs was averaged and the mean number of OHSt$^+$–RGCs per area unit was extrapolated to the total area of each retina (see below) to estimate the total number of OHSt$^+$–RGCs present in each one.

The *t*-test (SigmaStat® for Windows™ Version 3.11; Systat Software, Inc., Richmond, CA, USA) was used to compare the number of OHSt$^+$–RGCs in naïve or control uninjured right retinas with the axotomized left retinas. Differences were considered significant when $P < 0.05$.

3. Results

3.1. ERGs in control albino and pigmented mice

To study the effect of ONT on ERG waves in albino and pigmented mice, and as baseline measurements, simultaneous ERG recordings were performed from right and left eyes of each animal prior to surgery. Fig. 1 shows a representative example of the ERG traces recorded in an albino (Fig. 1A) and pigmented (Fig. 1B) mouse in response to flash stimuli of increasing intensity. The scotopic threshold responses (STR) were elicited by weak light stimuli (−6.26 to −4.02 log cd s m^{-2}).

The amplitudes of pSTR and nSTR increased exponentially with the intensity of the light stimulus both in albino and pigmented mice (Fig. 2A and B). No ERG *a*-wave was observed for light intensities below −2.36 log cd s m^{-2} (Fig. 1). The *b*-wave elicited by light

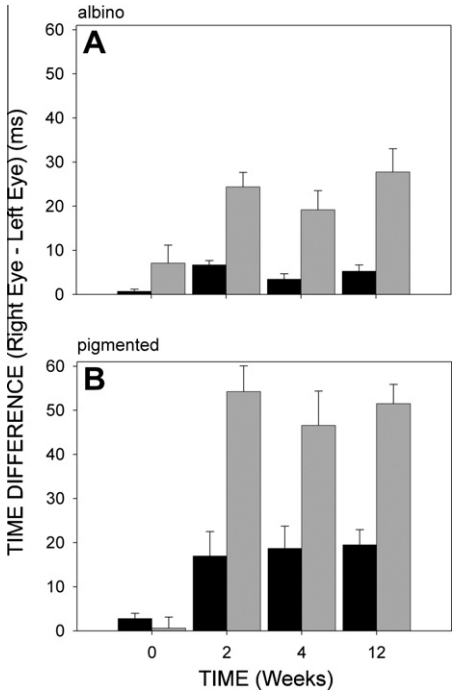

Fig. 6. STR implicit time-course. Average data (mean ± SEM) of the difference between right and left eye of the implicit time of nSTR (gray columns) and of pSTR (black columns) for albino (A) and pigmented (B) animals analyzed prior to and 2, 4 and 12 weeks after ONT. We observe an increase of the difference of the STR-implicit time between both eyes after ONT for both strains and STR components (*t*-test; $P < 0.05$), mainly for the nSTR component.

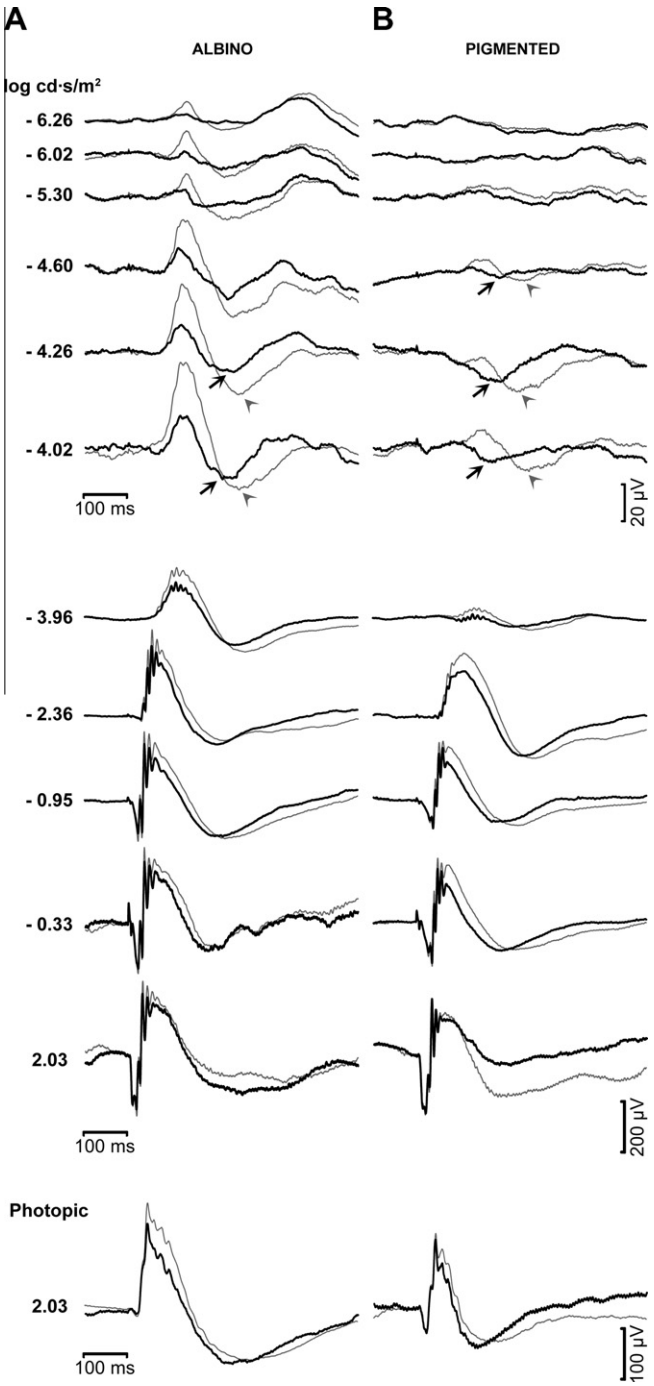

Fig. 7. Scotopic and photopic electroretinographic recordings 4 weeks after optic nerve transection. Examples of the ERG traces recorded in an albino (A) and pigmented (B) mouse in response to flash stimuli of increasing intensity for the non-operate right eye (thin traces) and for the operate left eye (bold traces) 4 weeks after the ONT. The intensity of the flash stimuli is indicated to the left of the recording traces. Reduction in the nSTR and pSTR responses from operated eyes versus control eyes is clearly observed for both strains. The STR-implicit time of the operated eye (arrows) is also altered respect to the non-operated eye (arrow heads). The *a*- and *b*-wave of the operated eye is slightly decreased respect to the non-operated eye.

intensities from -3.96 cd s m^{-2} increase exponentially, reaching its maximum for 2.03 cd s m^{-2} (Fig. 1). Fig. 2C and D shows averaged data of ERG *a*- and *b*-wave amplitudes in albino or pigmented mice, respectively. No significant differences in any of the above mentioned ERG amplitudes between left and right eyes were observed in any of the animals of this study prior to surgery. When the amplitudes obtained from the albino group were compared to those of the pigmented, there were no significant differences (*t*-test; $P > 0.05$) for all the waves analyzed except for the pSTR (*t*-test; $P < 0.05$).

3.2. ERGs in experimental albino and pigmented mice with left ONT

ERG recordings were performed simultaneously from right non-operated eye and left operated eye in albino and pigmented mice at increasing survival intervals after ONT.

3.2.1. Two weeks after ONT

Representative ERG traces from an albino mice in group I ($n = 9$) recorded from operated (bold trace) and non-operated (thin trace) eyes 2 weeks after left ONT are shown in Fig. 3A. The remained response for the pSTR and nSTR from operated eyes amounted to 40% of their fellow control eyes (Fig. 4A) (*t*-test, $P < 0.001$), and these are clearly observed at 2 weeks after ONT (Fig. 3A). At this time, scotopic and mixed ERG recorded in operated eyes also showed reduced *a*- and *b*-wave amplitudes with respect to control eye (Fig. 4C) (*t*-test, $P < 0.001$). Averaged data of ERG wave amplitudes from animals in group I is shown in Fig. 5A and C. Moreover, the implicit time of the pSTR and nSTR was reduced significantly when compared to the contralateral eye (ANOVA on Ranks; $P < 0.05$) (Fig. 6A), this difference was more marked for the nSTR (arrows and arrow heads in Figs. 3A and 6A).

Fig. 3B shows ERG traces from a representative pigmented mice in group IV ($n = 7$) recorded from operated (bold trace) and non-operated (thin trace) eyes 2 weeks after the ONT. The remained response for the pSTR and nSTR from operated eyes amounted to 30% and 65%, respectively, of their control eyes (Fig. 4B) (*t*-test, $P < 0.001$). At this time, scotopic and mixed ERG recorded in operated eye also showed slight reduced *a*- and *b*-wave amplitudes with respect to control eye (Fig. 4D) (*t*-test, $P < 0.001$). Averaged data of ERG wave amplitudes from animals in group IV is shown in Fig. 5B and D. Moreover, the implicit time of the pSTR and nSTR was reduced significantly when compared to the contralateral eye (ANOVA on ranks; $P < 0.05$); and this difference was more marked than that observed in albino mice (arrows and arrow heads in Figs. 3B and 6B).

3.2.2. Four weeks after ONT

Four weeks after ONT, differences of ERG wave amplitudes between operated and control eyes were also appreciated in group II ($n = 6$) of albino mice. Fig. 7A shows the ERG traces from a single representative animal of group II illustrating the remained response for the pSTR and nSTR of approximately 30% and 50%, respectively, in the operated eyes with respect to the control eyes (Fig. 4A) (*t*-test, $P < 0.001$). Moreover, the implicit time of the pSTR and nSTR was reduced significantly with respect to the contralateral eye (ANOVA on ranks; $P < 0.05$), (arrows and arrow heads in Figs. 7A and 6A). At this time, there was also a mild reduction of the ERG wave amplitudes observed for the scotopic and mixed responses, of an 80% approximately (Fig. 4C). Averaged data of ERG wave amplitudes from animals in group III is shown in Fig. 8A and C.

Four weeks after ONT, differences between ERG wave amplitudes among operated and control eyes were also appreciated in group V ($n = 6$) of pigmented mice. Fig. 7B shows the ERG traces from a single representative animal of group V illustrating the remained response for the pSTR and nSTR of approximately 25% and 70%, respectively, in the operated eyes with respect to the control eyes (Fig. 4B) (*t*-test, $P < 0.001$). Moreover, the implicit time of the pSTR and nSTR was reduced significantly compared to the contralateral eye (ANOVA on ranks; $P < 0.05$), and this reduction was more significant than that shown for the albino mice (arrows and

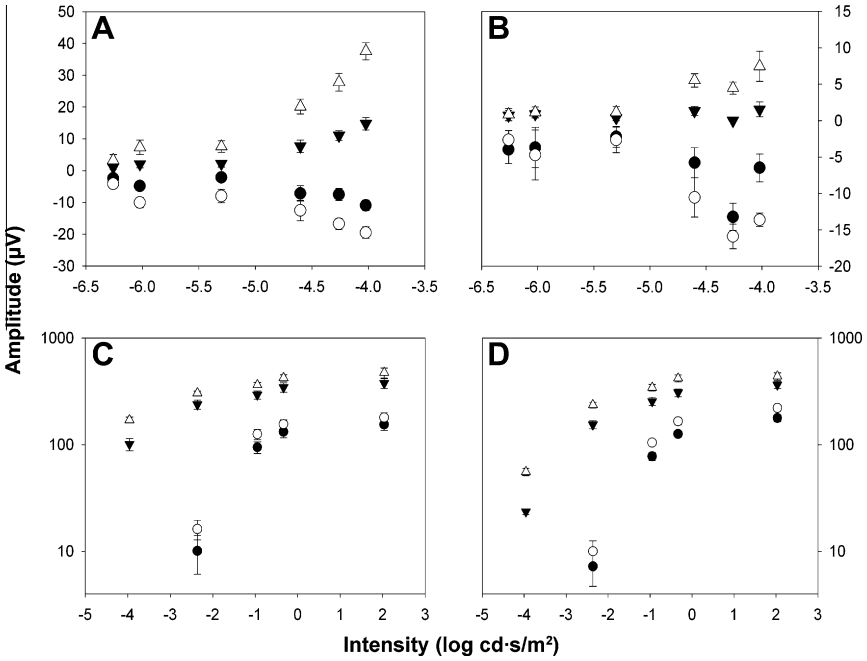

Fig. 8. Electroretinographic amplitude measurements 4 weeks after optic nerve transection. Averaged data (mean ± SEM) of ERG amplitudes versus stimulus intensity both from albino (A and C; $n = 6$) and pigmented mice (B and D; $n = 6$) from recordings obtained 4 weeks after ONT from non-operated right eyes (open symbols) and operated left eyes (filled symbols). (A and B) negative scotopic threshold responses (circles) and positive scotopic threshold responses (triangles). (C and D) *a*-wave (circles) and *b*-wave (triangles). A significant reduction of the wave amplitudes of the nSTR and pSTR is observed in the operated eyes (*t*-test; $P < 0.05$). Moreover, a mild decrease in the *b*-wave scotopic response and *a*- and *b*-wave is also observed in the operated eyes (*t*-test; $P < 0.05$) versus control eyes.

arrow heads in Figs. 7B and 6B). At this time, scotopic and mixed ERG recorded in the operated eyes also showed a mild reduction of the *a*- and *b*-wave amplitudes with respect to the control eye, of approximately an 80%, (Fig. 4D) (*t*-test, $P < 0.001$). Averaged data of ERG wave amplitudes from animals in group V is shown in Fig. 8B and D.

3.2.3. Twelve weeks after ONT

Twelve weeks after the ONT, changes in ERG wave amplitudes were still appreciated in operated eyes from group III of albino mice ($n = 5$) (Fig. 9A). At this time point after ONT, the remained response for the pSTR and nSTR from operated eyes represented approximately 50% and 70%, respectively, of the values recorded for the contralateral eyes (Fig. 4A) (*t*-test, $P < 0.001$), while a slight difference, of a 90% approximately, in the ERG scotopic and mixed responses was observed between operated and non-operated eyes (Fig. 4C). Averaged data of ERG wave amplitudes from animals in group III is shown in Fig. 10A and C. The implicit time of the pSTR and nSTR was maintained reduced significantly with respect to the contralateral eye (ANOVA on ranks; $P < 0.05$), (arrows and arrow heads in Figs. 9A and 6A).

In pigmented mice, 12 weeks after the ONT, changes in ERG wave amplitudes were still appreciated in operated eyes from group VI ($n = 9$) (Fig. 9B). At this time point after ONT, the remained response for the pSTR and nSTR from operated eyes amounted to approximately 50% respect to the values recorded for the contralateral eyes (Fig. 4C) (*t*-test, $P < 0.001$), while a mild difference, of an 80% approximately, in the ERG scotopic and mixed responses were observed between operated and non-operated eyes (Fig. 4D). Averaged data of ERG wave amplitudes from animals in group VI is shown in Fig. 10B and D. The implicit time of the pSTR and nSTR was also reduced significantly compared to the contralateral eye (ANOVA on ranks; $P < 0.05$). As shown at earlier time points, the reduction in the implicit time of these two waves, was statistically more significant in the pigmented than in the albino mice (arrows and arrow heads in Figs. 9B and 6B).

Our data demonstrates that reductions in the pSTR and nSTR are maintained long time after ONT and thus appear permanent both for albino and pigmented mice (Fig. 4A and B). However, the changes observed in the *a*- and *b*-wave amplitudes of the scotopic and mixed ERG are less obvious at any time after surgery (Fig. 4C and D).

3.3. Quantitative study of RGCs surviving after ONT

Fluorescence microscopy of whole-mounted naïve or contralateral control right retinas showed the normal appearance of $OHSt^+$–labeled RGCs typically distributed throughout the retina, as previously reported by our Laboratory for pigmented mice (Salinas-Navarro, Jiménez-López, et al., 2009) (Fig. 11A). The total population of RGCs was determined with an automatic routine in naïve or control retinas, and the total numbers of $OHSt^+$–RGCs were $39{,}447 \pm 2784$ (mean ± SD; $n = 8$) or $37{,}485 \pm 3766$ ($n = 8$), respectively. However, in the axotomized retinas, in addition to $OHSt^+$–RGCs there were also microglial cells (Fig. 11B), and this precluded automatic counting of RGCs. Manual counts of $OHSt^+$–RGCs allowed to estimate the total population of $OHSt^+$–RGCs which had diminished to 6639 ± 889 ($n = 8$), which is approximately an 18% of the RGC population found in their contralateral right uninjured retinas (Fig. 11C).

4. Discussion

Previous studies in adult rats have quantified the time-course and amount of RGC loss (Nadal-Nicolás et al., 2009; Parrilla-Reverter, Agudo, Sobrado-Calvo, et al., 2009; Peinado-Ramón et al., 1996; Sobrado-Calvo, Vidal-Sanz, & Villegas-Pérez, 2007; Villegas-Pérez et al., 1993) as well as the ERG alterations (Alarcón-Martínez et al., 2009; Bui & Fortune, 2004) that follow optic nerve transection (ONT). In small rodents, such as mice,

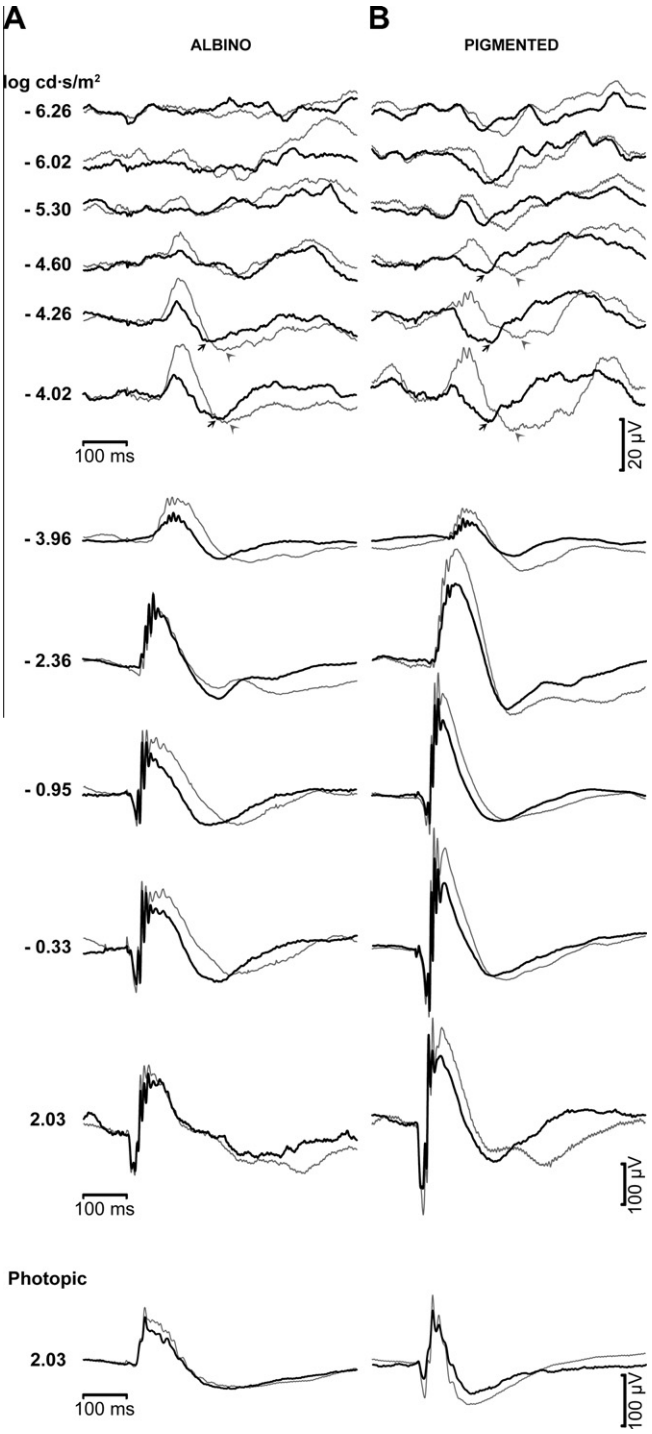

Fig. 9. Scotopic and photopic electroretinographic recordings 12 weeks after optic nerve transection. Examples of the ERG traces recorded in an albino (A) and pigmented (B) mouse in response to flash stimuli of increasing intensity for the non-operate right eye (thin traces) and for the operate left eye (bold traces) 12 weeks after the ONT. The intensity of the flash stimuli is indicated to the left of the recording traces. Reduction in the nSTR and pSTR responses from operated eyes versus control eyes is clearly observed 12 weeks after ONT for both mice strains. The STR-implicit time of the operated eye (arrows) is also altered respect to the non-operated eye (arrow heads). The *a*- and *b*-wave of the operated eye is slightly decreased respect to non-operated eye.

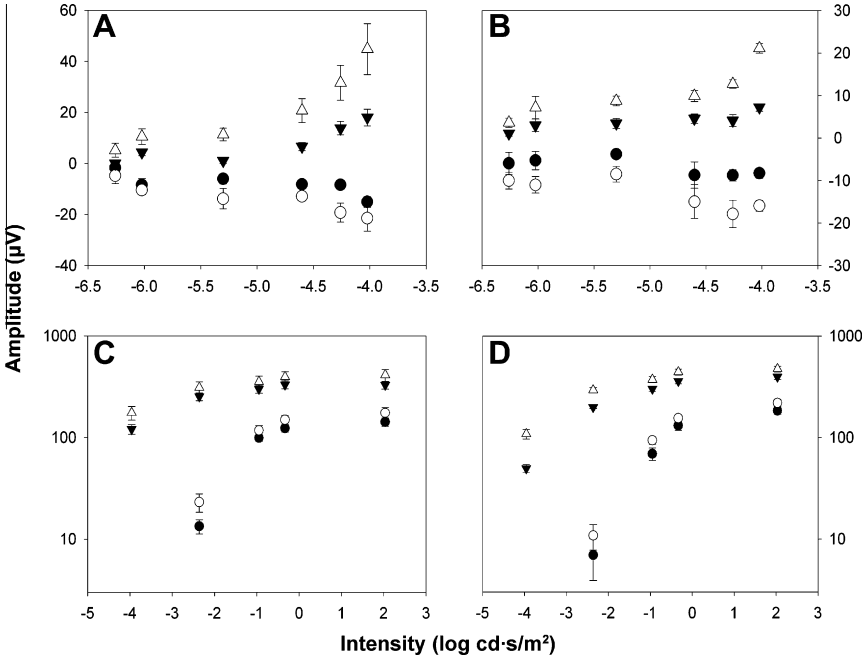

Fig. 10. Electroretinographic amplitude measurements 12 weeks after optic nerve transection. Averaged data (mean ± SEM) of ERG amplitudes versus stimulus intensity both from albino (A and C; $n = 5$) and pigmented mice (B and D; $n = 9$) from recordings obtained 12 weeks after ONT from non-operated right eyes (open symbols) and operated left eyes (filled symbols). (A and B) negative scotopic threshold response (circles) and positive scotopic threshold responses (triangles). (C and D) *a*-wave (circles) and *b*-wave (triangles). A significant reduction of the wave amplitudes of the nSTR and pSTR is observed in the operated eyes (*t*-test; $P < 0.05$). Moreover, a mild decrease in the *b*-wave scotopic response and *a*- and *b*-wave is maintained for the operated eyes (*t*-test; $P < 0.05$) versus control eyes.

ONT entails technical difficulties and this may explain why there are no anatomical studies investigating the time-course and amount of RGC loss (Galindo-Romero et al., 2010) neither their functional correlates following ONT. There are two studies reporting functional (Saszik et al., 2002) or anatomical (Kilic, Hermann, Isenmann, & Bähr, 2002) responses of mice retina after ON crush. Here we have performed a complete intraorbital optic nerve transection in albino and pigmented mice and have analyzed the retinal functionality prior to and at 2, 4 or 12 weeks after ONT of both eyes simultaneously. Moreover, using the retrogradely transported tracer OHSt applied to both superior colliculi, 1 week prior to axotomy to identify RGCs, we have also quantified RGCs surviving ONT at 2 weeks. We show that by 2 weeks after ONT there is a massive loss of RGCs (82% approximately) and this is associated with a prominent and persistent decrease in the amplitude of the STR components of the ERG, thus highlighting its importance as a functional correlate to assess the RGC population.

As in previous studies in the adult rat following ONT (Alarcón-Martínez et al., 2009; Bui & Fortune, 2004; Mojumder et al., 2008), we have also observed functional changes in the albino and pigmented mice ERG after ONT. Both components of the STR, but mainly the positive one, showed a reduction of their amplitude. The amplitude of pSTR in both mice strains had diminished to approximately 40% of their contralateral eye values, and these diminutions persisted along the time-course of our study. The nSTR amplitude was more variable between animals and showed a smaller diminution, especially in the albino animals, thus overall our data further suggests that in mice the pSTR component of the ERG results more affected after RGC damage. This is in accordance with a study in Math5/Brn3b double knock-out mice where there was a higher decrease of the positive component of the STR respect to the negative one (Moshiri et al., 2008). Other studies have shown an important diminution of the STR components following RGC damage in mice (Holcombe et al., 2008; Kong, Crowston, Vingrys, Trounce, & Bui, 2009; Salinas-Navarro, Alarcón-Martínez, et al., 2009) or rats (Alarcón-Martínez et al., 2009; Bui, Edmunds, Cioffi, & Fortune, 2005; Bui & Fortune, 2004; Fortune et al., 2004; He, Bui, & Vingrys, 2006), or after abolishment of the inner retinal neuron action potentials by pharmacological agents as GABA and NMDA (N-methyl-d-aspartate) in mice (Saszik et al., 2002) or NMDA (Bui & Fortune, 2004; Naarendorp, Sato, Cajdric, & Hubbard, 2001) and tetrodotoxin (TTX) in rats (Bui & Fortune, 2004).

A major decrease of the STR amplitude was first recorded 2 weeks after ONT, at a time when the survival of $OHSt^{+}$–RGCs is of approximately 18% of the control RGC population. Such a dramatic and rapid loss of RGCs after ON transection has been previously shown in the adult albino rat (Nadal-Nicolás et al., 2009; Peinado-Ramón et al., 1996; Vidal-Sanz et al., 2000; Villegas-Pérez et al., 1993) and mice ONT (Galindo-Romero et al., 2010). Moreover, the reductions of STR amplitudes were permanent for both strains of mice because by 12 weeks after the ONT these were still markedly reduced, suggesting a correlation between massive RGC loss and significant decreases of the STR amplitudes.

As shown in our previous work in albino and pigmented rat (Alarcón-Martínez et al., 2009), in the present studies there was also a residual response for the STR components after ONT. Further studies will have to analyze the origin of this residual ERG response, which at present is uncertain. RGCs surviving ONT could be responsible for the STR residual response, although this is unlikely because less than 18% of the RGC population survive ON axotomy in the adult rat (Berkelaar, Clarke, Wang, Bray, & Aguayo, 1994; Villegas-Pérez et al., 1993) or mice (Galindo-Romero et al., 2010). In addition to RGCs, other neuronal populations, such as the amacrine cells, which apparently are not directly affected by ONT (Carter et al., 1987; Schremser & Williams, 1992; Villegas-Pérez et al., 1993), could be responsible for the residual STR, as has been shown in other species such as cat and human (Sieving, 1991), and in transgenic mice lacking RGCs (Brzezinski et al., 2005). We cannot discard the possibility that other retinal neurons such as the bipolar could also contribute to the residual STR after ONT. Our results also show that after ONT there is a decrease of

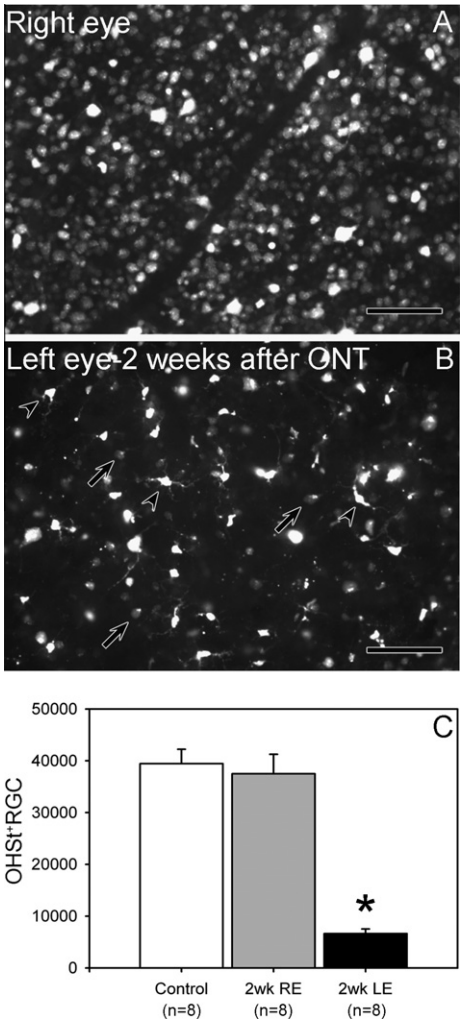

Fig. 11. Axotomy induces RGC death. Optic nerve transection (ONT) induces the death in RGCs as demonstrated by decrease of the OHSt$^+$RGCs population. (A and B) OHSt$^+$RGCs images from flat mounted retinas corresponding to an uninjured (right eye) (A) and to an experimental retina (left eye) analyzed 2 weeks after ONT (B). Two weeks after ONT, there is massive loss of OHSt$^+$RGCs (arrows) and there is presence of microglial cells transcellularly labeled with OHSt (arrow heads). Bar = 100 μm (C). Total number (mean ± SD) of OHSt$^+$RGCs in naïve (n = 8) (white column), untouched (right eyes) (n = 8) (gray column) and injured retinas (left eyes) (n = 8) (black column) analyzed 2 weeks after ONT. There is a significant decrease in the population of OHSt$^+$RGCs 2 weeks after ONT with respect to the untouched right and naïve retinas (t-test; $^*P < 0.001$). There is no difference between the number of OHSt$^+$RGC quantified in naïve and untouched right eyes.

the implicit time of both STRs in the operated eye with respect to its fellow eye, which is more marked in pigmented than in albino animals (Fig. 5). This is in agreement with a previous study in pigmented rats where a decrease of the implicit time of the nSTR was shown after an injection of TTX (Bui & Fortune, 2004) and with a Brn3b knock-out mice study which presented a high reduction of the number of RGCs for this animals and a faster nSTR respect to the wild type animals (Moshiri et al., 2008). It is possible that the implicit time of the negative component of the STR appeared earlier because the wave was no longer counteracted in the ERG by a normally larger pSTR. Thus, the alteration of the STR-implicit time can be presented as another feature of the ERG after RGC loss.

Finally, a slight reduction in the main *a*- and *b*-waves was present in albino and pigmented mice at all time points studied after ONT. This is in agreement with results obtained in pigmented and albino rats with their ON transected (Alarcón-Martínez et al., 2009; Bui & Fortune, 2004; Gargini et al., 2004), in which both *a*- and *b*-waves were reduced to approximately 80–85% with respect to their control values. We do not have a clear explanation for the reductions of these amplitudes, but one possibility is an alteration in the impedance of retina after RGC loss that would result in a change of the shape of the ERG response, another possibility that cannot be completely discarded would be the retrograde transneuronal degeneration of first and second order neurons in the retina following ONT (Germain, Calvo, & De La Villa, 2004; Günhan-Agar, Kahn, & Chalupa, 2000; Kielczewski, Pease, & Quigley, 2005). Whatever the explanation for the persistent reduction in the main *a*- and *b*-waves of the scotopic ERG, it is possible that these inner retinal changes could reflect more distal retinal changes, such as those observed in the STR.

In a number of pathologies, such as glaucoma, RGCs are the main neuronal population injured, thus it is important to have techniques to examine RGC functionality in vivo. There are few functional techniques to assess the RGC population in vivo, including the multifocal ERG (Ball & Petry, 2000) or the pattern ERG (Ben-Shlomo et al., 2005), but these techniques have some experimental limitations as the subject has to maintain the fixation on a point or it has to be emetropized, respectively. Another ERG response that could be associated to inner retinal elements is the photopic negative response or PhNR. The PhNR is a photopic wave identified in humans (Colotto et al., 2000; Gari et al., 2009; Machida, Gotoh, et al., 2008; Viswanathan, Frishman, Robson, & Walters, 2001) and other animals as monkeys (Viswanathan, Frishman, Robson, Harwerth, & Smith, 1999) and rats (Li, Barnes, & Holt, 2005), but its association with RGCs is not certain, at least in rodents (Machida, Raz-Prag, Fariss, Sieving, & Bush, 2008; Mojumder et al., 2008); in fact, in a study in pigmented rats with their optic nerve cut there was no change in the PhNR associated with RGC loss (Mojumder et al., 2008). Our present studies in albino and pigmented mouse, as well as those of others on pigmented (Alarcón-Martínez et al., 2009; Bui & Fortune, 2004) and albino rats (Alarcón-Martínez et al., 2009) show the clear relation between the STR components of the ERG and the population of RGC, indicating that the STR could be a functional index to demonstrate in vivo RGC dysfunction in a number of experimental models involving RGC injury such as acute (Bui et al., 2005; He et al., 2006; Kong et al., 2009) or chronic increase of the intraocular pressure (Cuenca et al., 2010; Fortune et al., 2004; Holcombe et al., 2008; Li, Tay, Chan, & So, 2006; Salinas-Navarro, Alarcón-Martínez, et al., 2009). Moreover, there are not many functional techniques to assess the RGC population in vivo, including the multifocal ERG (Ball & Petry, 2000), the pattern ERG (Ben-Shlomo et al., 2005) or the visual evoked potential (Wang et al., 2010), thus highlighting the importance of the STR recordings to identify this population of neurons in the adult albino or pigmented mice retina.

In summary, we have examined the ONT-induced alterations in the STR components of the ERG in adult mice and showed a clear and persistent diminution of these components, mainly the pSTR, with time after ONT in the albino and pigmented mouse. Moreover, we have showed a decrease of the implicit time of the STR components for both strains of mice. Thus, overall, the progressive diminution in the amplitude of the STR waves observed shortly after ONT and its persistence 12 weeks later highlights the importance of the STR recordings as an electrophysiological tool for the assessment of RGC function in these laboratory animals. This functional approach could be of great interest for a number of animal models coursing with degeneration of the RGC population, for which up to date there are few tests to examine RGC function in vivo.

Acknowledgments

This work was supported by research grants from the Regional Government of Murcia; Fundación Séneca 05703/PI/07 (MPVP),

04446/GERM/07 (MVS); Spanish Ministry of Education and Science SAF-2009-10385 MVS); SAF2007-66175 (PdlV); and Spanish Ministry of Health ISCIII: FIS PIO06/0780 (MPVP), RD07/0062/0001 (MVS), RD07/0062/0008 (PdlV) and ISCIII-FEDER: PIO70225 (MAB);

References

Aguayo, A. J., Vidal-Sanz, M., Villegas-Pérez, M. P., & Bray, G. M. (1987). Growth and connectivity of axotomized retinal neurons in adult rats with optic nerves substituted by PNS grafts linking the eye and the midbrain. *Annals of the New York Academy of Sciences, 495*, 1–9.

Agudo, M., Pérez-Marín, M. C., Lonngren, U., Sobrado, P., Conesa, A., Cánovas, I., et al. (2008). Time course profiling of the retinal transcriptome after optic nerve transection and optic nerve crush. *Molecular Vision, 14*, 1050–1063.

Agudo, M., Pérez-Marín, M. C., Sobrado-Calvo, P., Lonngren, U., Salinas-Navarro, M., Canovas, I., et al. (2009). Proteins belonging to different branches of the apoptotic cascade are immediately up-regulated in the retina after optic nerve transection or optic nerve crush. *Investigative Ophthalmology Visual Science, 50*, 424–431.

Alarcón-Martínez, L., Avilés-Trigueros, M., De la Villa, P., Valiente-Soriano, J., Salinas-Navarro, M., Sánchez-Migallón Carreras, M. C., et al. (2010). Short and long term axotomy-induced erg changes in albino and pigmented mice. *Investigative Ophthalmology and Visual Science, 51* (E-abstract 5566).

Alarcón-Martínez, L., De la Villa, P., Avilés-Trigueros, M., Blanco-Velasco, R., Villegas-Pérez, M. P., & Vidal-Sanz, M. (2009). Short and long term axotomy-induced ERG changes in albino and pigmented rats. *Molecular Vision, 15*, 2373–2383.

Avilés-Trigueros, M., Sauvé, Y., Lund, R. D., & Vidal-Sanz, M. (2000). Selective innervation of retinorecipient brainstem nuclei by retinal ganglion cell axons regenerating through peripheral nerve grafts in adult rats. *Journal of Neuroscience, 20*, 361–374.

Ball, S. L., & Petry, H. M. (2000). Noninvasive assessment of retinal function in rats using multifocal electroretinography. *Investigative Ophthalmology and Visual Science, 41*, 610–617.

Ben-Shlomo, G., Bakalash, S., Lambrou, G. N., Latour, E., Dawson, W. W., Schwartz, M., et al. (2005). Pattern electroretinography in a rat model of ocular hypertension: Functional evidence for early detection of inner retinal damage. *Experimental Eye Research, 81*, 340–349.

Berkelaar, M., Clarke, D. B., Wang, Y. C., Bray, G. M., & Aguayo, A. J. (1994). Axotomy results in delayed death and apoptosis of retinal ganglion cells in adult rats. *Journal of Neuroscience, 14*, 4368–4374.

Brzezinski, J. A., 4th, Brown, N. L., Tanikawa, A., Bush, R. A., Sieving, P. A., Vitaterna, M. H., et al. (2005). Loss of circadian photoentrainment and abnormal retinal electrophysiology in Math5 mutant mice. *Investigative Ophthalmology and Visual Science, 46*, 2540–2551.

Bui, B. V., Edmunds, B., Cioffi, G. A., & Fortune, B. (2005). The gradient of retinal functional changes during acute intraocular pressure elevation. *Investigative Ophthalmology and Visual Science, 46*, 202–213.

Bui, B. V., & Fortune, B. J. (2004). Ganglion cell contributions to the rat full-field electroretinogram. *Physiology, 555*(Pt 1), 153–173.

Carter, D. A., Vidal-Sanz, M., & Aguayo, A. J. (1987). Long-term preservation of intrinsic neurons after axotomy-induced death of retinal ganglion cells. *Society of Neuroscience Abstract, 13*, 1390.

Casson, R. J., Chidlow, G., Wood, J. P., Vidal-Sanz, M., & Osborne, N. N. (2004). The effect of retinal ganglion cell injury on light-induced photoreceptor degeneration. *Investigative Ophthalmology and Visual Science, 45*, 685–693.

Cheunsuang, O., & Morris, R. (2005). Astrocytes in the arcuate nucleus and median eminence that take up a fluorescent dye from the circulation express leptin receptors and neuropeptide Y Y1 receptors. *Glia, 52*, 228–233.

Chidlow, G., Casson, R., Sobrado-Calvo, P., Vidal-Sanz, M., & Osborne, N. N. (2005). Measurement of retinal injury in the rat after optic nerve transection: An RT-PCR study. *Molecular Vision, 11*, 387–396.

Colotto, A., Falsini, B., Salgarello, T., Iarossi, G., Galan, M. E., & Scullica, L. (2000). Photopic negative response of the human ERG: Losses associated with glaucomatous damage. *Investigative Ophthalmology and Visual Science, 41*, 2205–2211.

Cuenca, N., Pinilla, I., Fernández-Sánchez, L., Salinas-Navarro, M., Alarcón-Martínez, L., Avilés-Trigueros, M., et al. (2010). Changes in the inner and outer retinal layers after acute increase of the intraocular pressure in adult albino swiss mice. *Experimental Eye Research, 9*, 273–285.

Dowling, J. E. (1987). *The Retina. An approachable part of the brain*. Cambridge, Massachusetts, and London, England: The Belknap Press of Harvard University Press.

Fortune, B., Bui, B. V., Morrison, J. C., Johnson, E. C., Dong, J., Cepurna, W. O., et al. (2004). Selective ganglion cell functional loss in rats with experimental glaucoma. *Investigative Ophthalmology and Visual Science, 45*, 1854–1862.

Frishman, L. J. (2006). Origins of the electroretinogram. In John R. Heckenlively & Geoffrey B. Arden (Eds.), *Principles and practice of clinical electrophysiology of vision* (2nd ed., pp. 139–184). Cambridge, Massachusetts and London, England: Massachusetts Institute of Technology (MIT).

Frishman, L. J., Reddy, M. G., & Robson, J. G. (1996). Effects of background light on the human dark-adapted ERG and psychophysical threshold. *Journal of the Optical Society of America A. Optics and Image Science, 13*, 601–612.

Frishman, L. J., Shen, F. F., Du, L., Robson, J. G., Harwerth, R. S., Smith, E. L. 3rd,, et al. (1996). The scotopic electroretinogram of macaque after retinal ganglion cell loss from experimental glaucoma. *Investigative Ophthalmology and Visual Science, 37*, 125–141.

Frishman, L. J., & Steinberg, R. H. (1989a). Intraretinal analysis of the threshold dark-adapted ERG of cat retina. *Journal of Neurophysiology, 61*, 1221–1232.

Frishman, L. J., & Steinberg, R. H. (1989b). Light-evoked increases in [K+]o in proximal portion of the dark-adapted cat retina. *Journal of Neurophysiology, 61*, 1233–1243.

Fu, C. T., & Sretavan, D. (2010). Laser-induced ocular hypertension in albino CD-1 mice. *Investigative Ophthalmology and Visual Science, 51*, 980–990.

Galindo-Romero, C., Avilés-Trigueros, M., Jiménez-López, M., Valiente-Soriano, F., Nadal-Nicolás, F., Rodriguez-Llarena, S., et al. (2010). Time course of retinal ganglion cell degeneration in adult mice after optic nerve axotomy. *Investigative Ophthalmology and Visual Science, 51* (ARVO E-abstract 637).

Gargini, C., Bisti, S., Demontis, G. C., Valter, K., Stone, J., & Cervetto, L. (2004). Electroretinogram changes associated with retinal upregulation of trophic factors: Observations following optic nerve section. *Neuroscience, 126*, 775–783.

Gari, M., Colotto, A., Salgarello, A., Fadda, A., Di Renzo, A., Anselmi, G., et al. (2009). Photopic negative response from retinal hemifields in glaucoma. *Investigative Ophthalmology and Visual Science, 50* (E-abstract 5302).

Germain, F., Calvo, M., & De La Villa, P. (2004). Rabbit retinal ganglion cell survival after optic nerve section and its effect on inner plexiform layer. *Experimental Eye Research, 79*, 95–102.

Gómez-Ramírez, A. M., Villegas-Pérez, M. P., Miralles de Imperial, J., Salvador-Silva, M., & Vidal-Sanz, M. (1999). Effects of intramuscular injection of botulinum toxin and doxorubicin on the survival of abducens motoneurons. *Investigative Ophthalmology and Visual Science, 40*, 414–424.

Grozdanic, S. D., Betts, D. M., Sakaguchi, D. S., Allbaugh, R. A., Kwon, Y. H., & Kardon, R. H. (2003). Laser-induced mouse model of chronic ocular hypertension. *Investigative Ophthalmology and Visual Science, 44*, 4337–4346.

Günhan-Agar, E., Kahn, D., & Chalupa, L. M. (2000). Segregation of on and off bipolar cell axonal arbors in the absence of retinal ganglion cells. *Journal of Neuroscience, 20*, 306–314.

He, A., Bui, B. V., & Vingrys, A. J. (2006). The rate of functional recovery from acute IOP elevation. *Investigative Ophthalmology and Visual Science, 47*, 4872–4880.

Holcombe, D. J., Lengefeld, N., Gole, G. A., & Barnett, N. L. (2008). Selective inner retinal dysfunction precedes ganglion cell loss in a mouse glaucoma model. *British Journal of Ophthalmology, 92*, 683–688.

Kielczewski, J. L., Pease, M. E., & Quigley, H. A. (2005). The effect of experimental glaucoma and optic nerve transection on amacrine cells in the rat retina. *Investigative Ophthalmology and Visual Science, 46*, 3188–3196.

Kilic, E., Hermann, D. M., Isenmann, S., & Bähr, M. (2002). Effects of pinealectomy and melatonin on the retrograde degeneration of retinal ganglion cells in a novel model of intraorbital optic nerve transection in mice. *Journal of Pineal Research, 32*, 106–111.

Kong, Y. X., Crowston, J. G., Vingrys, A. J., Trounce, I. A., & Bui, V. B. (2009). Functional changes in the retina during, after acute intraocular pressure elevation in mice. *Investigative Ophthalmology and Visual Science, 50*, 5732–5740.

Korth, M., Nguyen, N. X., Horn, F., & Martus, P. (1994). Scotopic threshold response and scotopic PII in glaucoma. *Investigative Ophthalmology and Visual Science, 35*, 619–625.

Li, B., Barnes, G. E., & Holt, W. F. (2005). The decline of the photopic negative response (PhNR) in the rat after optic nerve transection. *Documenta Ophthalmologica, 111*, 23–31.

Li, R. S., Tay, D. K., Chan, H. H., & So, K. F. (2006). Changes of retinal functions following the induction of ocular hypertension in rats using argon laser photocoagulation. *Clinical and Experimental Ophthalmology, 34*, 575–583.

Lindqvist, N., Lönngren, U., Agudo, M., Näpänkangas, U., Vidal-Sanz, M., & Hallböök, F. (2010). Multiple receptor tyrosine kinases are expressed in adult rat retinal ganglion cells as revealed by single-cell degenerate primer polymerase chain reaction. *Upsala Journal of Medical Sciences, 115*, 65–80.

Lindqvist, N., Peinado-Ramónn, P., Vidal-Sanz, M., & Hallböök, F. (2004). GDNF, Ret, GFR alpha 1 and 2 in the adult retino-tectal system after optic nerve transection. *Experimental Neurology, 187*, 487–499.

Lindqvist, N., Vidal-Sanz, M., & Hallböök, F. (2002). Single cell RT-PCR analysis of tyrosine kinase receptor expression in adult rat retinal ganglion cells isolated by retinal sandwiching. *Brain Research and Brain Research Protocols, 10*, 75–83.

Machida, S., Gotoh, Y., Toba, Y., Ohtaki, A., Kaneko, M., & Kurosaka, D. (2008). Correlation between photopic negative response and retinal nerve fiber layer thickness and optic disc topography in glaucomatous eyes. *Investigative Ophthalmology and Visual Science, 49*, 2201–2207.

Machida, S., Raz-Prag, D., Fariss, R. N., Sieving, P. A., & Bush, R. A. (2008). Photopic ERG negative response from amacrine cell signaling in RCS rat retinal degeneration. *Investigative Ophthalmology and Visual Science, 49*, 442–452.

McKerracher, L., Vidal-Sanz, M., & Aguayo, A. J. (1990). Slow transport rates of cytoskeletal proteins change during regeneration of axotomized retinal neurons in adult rats. *Journal of Neuroscience, 10*, 641–648.

McKerracher, L., Vidal-Sanz, M., Essagian, C., & Aguayo, A. J. (1990). Selective impairment of slow axonal transport after optic nerve injury in adult rats. *Journal of Neuroscience, 10*, 2834–2841.

Mojumder, D. K., Sherry, D. M., & Frishman, L. J. (2008). Contribution of voltage-gated sodium channels to the *b*-wave of the mammalian flash electroretinogram. *Journal of Physiology, 586*, 2551–2580.

Morrison, J. C., Johnson, E., & Cepurna, W. O. (2008). Rat models for glaucoma research. *Progress in Brain Research, 173*, 285–301.

Moshiri, A., Gonzalez, E., Tagawa, K., Maeda, H., Wang, M., Frishman, L. J., et al. (2008). Near complete loss of retinal ganglion cells in the math5/brn3b double knockout elicits severe reductions of other cell types during retinal development. *Developmental Biology, 316*, 214–227.

Naarendorp, F., Sato, Y., Cajdric, A., & Hubbard, N. P. (2001). Absolute and relative sensitivity of the scotopic system of rat: Electroretinography and behavior. *Visual Neuroscience, 18*, 641–656.

Naarendorp, F., & Sieving, P. A. (1991). The scotopic threshold response of the cat ERG is suppressed selectively by GABA and glycine. *Vision Research, 31*, 1–15.

Nadal-Nicolás, F. M., Jiménez-López, M., Sobrado-Calvo, P., Nieto-López, L., Cánovas-Martínez, I., Salinas-Navarro, M., et al. (2009). Brn3a as a marker of retinal ganglion cells: Qualitative and quantitative time course studies in naive and optic nerve-injured retinas. *Investigative Ophthalmology and Visual Science, 50*, 3860–3868.

Parrilla-Reverter, G., Agudo, M., Nadal-Nicolás, F., Alarcón-Martínez, L., Jiménez-López, M., Salinas-Navarro, M., et al. (2009). Time-course of the retinal nerve fibre layer degeneration after complete intra-orbital optic nerve transection or crush: A comparative study. *Vision Research, 49*, 2808–2825.

Parrilla-Reverter, G., Agudo, M., Sobrado-Calvo, P., Salinas-Navarro, M., Villegas-Pérez, M. P., & Vidal-Sanz, M. (2009). Effects of different neurotrophic factors on the survival of retinal ganglion cells after a complete intraorbital nerve crush injury: A quantitative in vivo study. *Experimental Eye Research, 89*, 32–41.

Peinado-Ramón, P., Salvador, M., Villegas-Pérez, M. P., & Vidal-Sanz, M. (1996). Effects of axotomy and intraocular administration of NT-4, NT-3, and brain-derived neurotrophic factor on the survival of adult rat retinal ganglion cells. A quantitative in vivo study. *Investigative Ophthalmology and Visual Science, 37*, 489–500.

Robson, J. G., & Frishman, L. J. (1995). Response linearity and kinetics of the cat retina: The bipolar cell component of the dark-adapted electroretinogram. *Visual Neuroscience, 12*, 837–850.

Salinas-Navarro, M., Alarcón-Martínez, L., Valiente-Soriano, F. J., Jiménez-López, M., Mayor-Torroglosa, S., Avilés-Trigueros, M., et al. (2010). Ocular hypertension impairs optic nerve axonal transport leading to progressive retinal ganglion cell degeneration. *Experimental Eye Research, 90*, 168–183.

Salinas-Navarro, M., Alarcón-Martínez, L., Valiente-Soriano, F. J., Ortín-Martínez, A., Jiménez-López, M., Avilés-Trigueros, M., et al. (2009). Functional and morphological effects of laser-induced ocular hypertension in adult albino swiss mice retina. *Molecular Vision, 15*, 2578–2598.

Salinas-Navarro, M., Jiménez-López, M., Valiente-Soriano, F., Alarcón-Martínez, L., Avilés-Trigueros, M., Mayor-Torroglosa, S., et al. (2009). Retinal ganglion cell population in adult albino and pigmented mice: A computerised analysis of the entire population and its spatial distribution. *Vision Research, 49*, 636–646.

Salinas-Navarro, M., Mayor-Torroglosa, S., Jiménez-López, M., Avilés-Trigueros, M., Holmes, T. M., Lund, R. D., et al. (2009). A computerized analysis of the entire retinal ganglion cell population and its spatial distribution in adult rats. *Vision Research, 49*, 115–126.

Salvador-Silva, M., Vidal-Sanz, M., & Villegas-Pérez, M. P. (2000). Microglial cells in the retina of *Carassius auratus*: Effects of optic nerve crush. *Journal of Comparative Neurology, 417*, 431–447.

Saszik, S., Frishman, L. J., & Robson, J. G. (2002). The scotopic threshold response of the dark-adapted electroretinogram of the mouse. *Journal of Physiology, 543*, 899–916.

Schlamp, C. L., Johnson, E. C., Li, Y., Morrison, J. C., & Nickells, R. W. (2001). Changes in Thy1 gene expression associated with damaged retinal ganglion cells. *Molecular Vision, 7*, 192–201.

Schremser, J. L., & Williams, T. P. (1992). Photoreceptor plasticity in the albino rat retina following unilateral optic nerve section. *Experimental Eye Research, 55*, 393–399.

Sieving, P. A. (1991). Retinal ganglion cell loss does not abolish the scotopic threshold response (STR) of the cat and human ERG. *Clinical Vision Science, 2*, 149–158.

Sieving, P. A., Frishman, L. J., & Steinberg, R. H. (1986). Scotopic threshold response of proximal retina in cat. *Journal of Neurophysiology, 56*, 1049–1061.

Sieving, P. A., & Nino, C. (1988). Human scotopic threshold response. *Investigative Ophthalmology and Visual Science, 29*, 1608–1614.

Sobrado-Calvo, P., Vidal-Sanz, M., & Villegas-Pérez, M. P. (2007). Rat retinal microglial cells under normal conditions, after optic nerve section, and after optic nerve section and intravitreal injection of trophic factors or macrophage inhibitory factor. *Journal of Comparative Neurology, 501*(6), 866–878.

Vidal-Sanz, M., Bray, G. M., & Aguayo, A. J. (1991). Regenerated synapses persist in the superior colliculus after the regrowth of retinal ganglion cell axons. *Journal of Neurocytology, 20*, 940–952.

Vidal-Sanz, M., Bray, G. M., Villegas-Perez, M. P., Thanos, S., & Aguayo, A. J. (1987). Axonal regeneration and synapse formation in the superior colliculus by retinal ganglion cells in the adult rat. *Journal of Neuroscience, 7*, 2894–2909.

Vidal-Sanz, M., Lafuente, M. P., Mayor, S., de Imperial, J. M., & Villegas-Pérez, M. P. (2001). Retinal ganglion cell death induced by retinal ischemia. Neuroprotective effects of two alpha-2 agonists. *Survey of Ophthalmology, 45*, 261–267.

Vidal-Sanz, M., Lafuente, M., Sobrado-Calvo, P., Sellés-Navarro, I., Rodríguez, E., Mayor-Torroglosa, S., et al. (2000). Death and neuroprotection of retinal ganglion cells after different types of injury. *Neurotoxicity Research, 2*, 215–227.

Vidal-Sanz, M., Villegas-Perez, M. P., Bray, G. M., & Aguayo, A. J. (1988). Persistent retrograde labeling of adult rat retinal ganglion cells with the carbocyanine dye dil. *Experimental Neurology, 102*, 92–101.

Vidal-Sanz, M., Villegas-Perez, M. P., Bray, G. M., & Aguayo, A. J. (1993). Use of peripheral nerve grafts to study regeneration after CNS injury. *Neuroprotocols, 3*, 29–33.

Villegas-Pérez, M. P., Vidal-Sanz, M., Bray, G. M., & Aguayo, A. J. (1988). Influences of peripheral nerve grafts on the survival and regrowth of axotomized retinal ganglion cells in adult rats. *Journal of Neuroscience, 8*, 265–280.

Villegas-Pérez, M. P., Vidal-Sanz, M., Rasminsky, M., Bray, G. M., & Aguayo, A. J. (1993). Rapid and protracted phases of retinal ganglion cell loss follow axotomy in the optic nerve of adult rats. *Journal of Neurobiology, 24*, 23–36.

Viswanathan, S., Frishman, L. J., Robson, J. G., Harwerth, R. S., & Smith, E. L. 3rd, (1999). The photopic negative response of the macaque electroretinogram: Reduction by experimental glaucoma. *Investigative Ophthalmology and Visual Science, 40*, 1124–1136.

Viswanathan, S., Frishman, L. J., Robson, J. G., & Walters, J. W. (2001). The photopic negative response of the flash electroretinogram in primary open angle glaucoma. *Investigative Ophthalmology and Visual Science, 42*, 514–522.

Wachtmeister, L. (1998). Oscillatory potentials in the retina: What do they reveal. *Progress in Retinal and Eye Research, 17*, 485–521.

Wang, S., Villegas-Pérez, M. P., Holmes, T., Lawrence, J. M., Vidal-Sanz, M., Hurtado-Montalbán, N., et al. (2003). Evolving neurovascular relationships in the RCS rat with age. *Current Eye Research, 27*, 183–196.

Wang, S., Villegas-Pérez, M. P., Vidal-Sanz, M., & Lund, R. D. (2000). Progressive optic axon dystrophy and vascular changes in rd mice. *Investigative Ophthalmology and Visual Science, 41*, 537–545.

Wang, R., Xu, J., Xie, J., Kang, Z., Sun, X., Chen, N., et al. (2010). Hyperbaric oxygen preconditioning promotes survival of retinal ganglion cells in a rat model of optic nerve crush. *Journal of Neurotrauma, 27*, 763–770.

Whiteley, S. J., Sauvé, Y., Avilés-Trigueros, M., Vidal-Sanz, M., & Lund, R. D. (1998). Extent and duration of recovered pupillary light reflex following retinal ganglion cell axon regeneration through peripheral nerve grafts directed to the pretectum in adult rats. *Experimental Neurology, 154*, 560–572.